Available online at www.sciencedirect.com

SciVerse ScienceDirect

journal homepage: www.elsevier.com/locate/ijrefrig

Single temperature sensor superheat control using a novel maximum slope-seeking method

K. Vinther [a,*], H. Rasmussen [a], R. Izadi-Zamanabadi [a,b], J. Stoustrup [a]

[a] Automation and Control, Department of Electronic Systems, Aalborg University, Fredrik Bajers Vej 7C, 9220 Aalborg, Denmark
[b] Electronic Controllers and Services, Danfoss A/S, L21 N14, Nordborgvej 81, 6430 Nordborg, Denmark

ARTICLE INFO

Article history:
Received 31 August 2012
Received in revised form
5 November 2012
Accepted 17 November 2012
Available online 23 November 2012

Keywords:
Refrigeration systems
Evaporator
Superheat
Maximum slope-seeking
Harmonics
Control

ABSTRACT

Superheating of refrigerant in the evaporator is an important aspect of safe operation of refrigeration systems. The level of superheat is typically controlled by adjusting the flow of refrigerant using an electronic expansion valve, where the superheat is calculated using measurements from a pressure and a temperature sensor. In this paper we show, through extensive testing, that the superheat or filling of the evaporator can actually be controlled using only a single temperature sensor. This can either reduce commissioning costs by lowering the necessary amount of sensors or add fault tolerance in existing systems if a sensor fails (e.g. pressure sensor). The solution is based on a novel maximum slope-seeking control method, where a perturbation signal is added to the valve opening degree, which gives additional information about the system for control purposes. Furthermore, the method does not require a model of the system and can be tuned automatically.

Régulation de la surchauffe à l'aide d'un capteur de température unique et une méthode innovante de recherche de la pente maximale de la courbe

Mots clés : systèmes frigorifiques ; évaporateur ; surchauffe ; recherche de la pente maximale de la courbe ; harmoniques ; régulation

1. Introduction

Refrigeration systems are a big part of our society. Typical examples range from small fridges and freezers in our homes to residential air conditioning systems and supermarket systems with multiple display cases. All these systems typically rely on a vapor compression cycle where refrigerant is evaporated in an evaporator, while extracting heat from the surroundings. Details of the refrigeration cycle is not given here (the reader is referred to references such as He et al.

* *Corresponding author*. Tel.: +45 20991661.
E-mail addresses: kv@es.aau.dk (K. Vinther), hr@es.aau.dk (H. Rasmussen), roozbeh@danfoss.com (R. Izadi-Zamanabadi), jakob@es.aau.dk (J. Stoustrup).
0140-7007/$ – see front matter © 2012 Elsevier Ltd and IIR. All rights reserved.
http://dx.doi.org/10.1016/j.ijrefrig.2012.11.018

Nomenclature

Acronyms

COP	Coefficient of Performance
EEV	Electronic expansion valve
FOPDT	First order plus dead time
I/O	Input/output
MSS	Maximum slope-seeking
PWM	Pulse-width modulation
TXV	Thermostatic expansion valve

Greek letters

Δ	Difference
ω	Angular frequency (rad s^{-1})
ϕ	Phase (°)
θ	Angle (°)
ξ	Error signal

Other symbols

$\bar{x}$	Average value of x
x^*	Desired operating point of x

Variables

$\mathscr{H}$	Hold operator
S	Sample operator
A	Amplitude
f	Frequency (Hz)
H	Harmonic
j	Imaginary unit
K	Integral gain
N	Sample size
n	Sample index
OD	Opening degree (%)
P	Pressure (bar)
s	Laplace domain variable
T	Temperature (°C) or time constant (s)
t	Time (s)
u	Control output or process input
y	System or process output
z	Frequency domain variable

Subscripts

a	Air
amb	Ambient
c	Condenser or condensation
conv	Conventional
cp	Compressor
ctrl	Control
d	Delay
dca	Display case air
df	Defrost
e	Evaporator or evaporation
ex	Excitation or perturbation
hvac	Heating ventilation and air conditioning
i	Inlet or input
mss	Maximum slope-seeking
n	Normalized
o	Outlet or output
r	Room
ref	Reference
s	Sample
sh	Superheat
sl	Safety logic
sub	Subcooling
sys	System
t	Threshold
txv	Thermostatic expansion valve
u	Ultimate
w	Water

(1998); Dincer and Kanoglu (2010)), but the cooling capacity of the system is in general increased in two ways: either by lowering the evaporation temperature or by having as much liquid refrigerant in the evaporator as possible (Elliott and Rasmussen, 2010). However, lowering of the evaporation temperature requires more compressor work and care must be taken not to let liquid refrigerant enter the compressor, as this can increase the wear and possibly damage it. After all refrigerant is evaporated into gas it will start to superheat and the level of superheat, T_{sh}, is an indirect measure of the filling of the evaporator. The superheat is calculated using a temperature sensor located at the outlet of the evaporator, $T_{e,o}$, and a pressure measurement that can be converted to the evaporation temperature, T_e, and it is typically controlled using an electronic expansion valve (EEV), where the opening degree (OD) of this valve determines the refrigerant flow (see e.g. Finn and Doyle (2000); Elliott and Rasmussen (2010)). This is shown in Fig. 1, where the input/output (I/O) map shows the qualitative connection between OD and temperature. Alternatively, the superheat can also be controlled with the compressor speed as in Rasmussen (2008) or a combination as in Schurt et al. (2009); He et al. (1998). However, using the compressor to control the superheat is not done in multi evaporator systems (they each have different flow requirements).

Pressure sensors are expensive to buy and install compared to temperature sensors; especially in multi

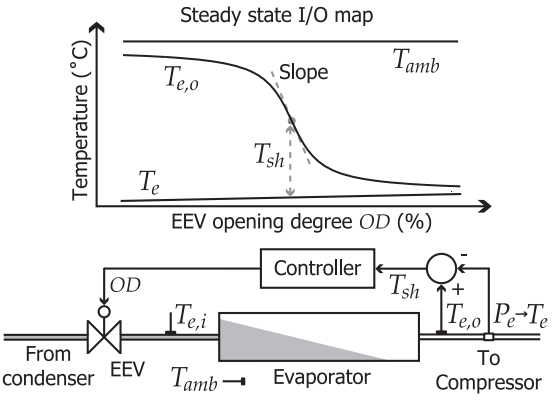

Fig. 1 – Evaporator steady state I/O map and typical superheat control using a pressure transducer, a temperature transducer, and an EEV.

evaporator systems with different evaporation pressures as multiple sensors are needed. An alternative is to use two temperature sensors instead ($T_{e,i}$ and $T_{e,o}$), since temperature transducers are cheaper. However, this also requires installation of at least two sensors and they could be placed incorrectly. Additionally, control relying on multiple sensors introduces multiple possible points of failure (sensor malfunction). We have therefore investigated the possibility of controlling the filling using only a single temperature sensor and an EEV. This could provide fault tolerant control possibilities in existing systems and potentially reduce commissioning costs by requiring fewer sensors.

The challenge is to extract enough information out of the single temperature measurement to be able to control the valve and the refrigerant flow. One possibility would be simply to use a fixed temperature reference. However, a suitable reference will depend on operating conditions, the type of refrigeration system in question, and disturbances, which is why a fixed reference is not a suitable solution (finding a suitable reference superheat in conventional two sensor control is also a challenge). An alternative is to use qualitative knowledge about the system and the behavior of the evaporator outlet temperature. A variance based control method was investigated in Vinther et al. (2012a), where it was discovered that the variance of the outlet temperature increased at low superheat, which can be used for feedback purposes. This is also closely related to the automatic variance control method (Moir, 2001), which in some cases has been used in the conventional two sensor superheat control to adjust the reference. A problem with the variance based method is its sensitivity to operating conditions and to large disturbances, as this can change the variance level.

One can also use continuous excitation to gain the required knowledge to control the system. Extremum and slope-seeking control are examples of this, where the objective is to drive the output to an extremum or certain slope in the system I/O map. These methods are well covered in Ariyur and Krstic (2003) and Zhang and Ordez (2012). Furthermore, Moase and Manzie (2011) and Henning et al. (2008) provides examples of faster observer based extremum-seeking and there exist multiple examples of the applicability of extremum and slope-seeking control. A refrigeration system example is given in Sane et al. (2006), where the total sum of cooling tower and chiller power consumption is minimized in a chilled water cooling plant, by optimization of the condenser water temperature with extremum-seeking (the I/O relation between power consumption and condenser water temperature is concave). A similar example is given in Li et al. (2012).

As we will show in this paper, the I/O map between evaporator valve OD and outlet temperature can be approximated by a smooth function, with sigmoid function properties, which is differentiable, and has a bell shaped non-positive first derivative (see Fig. 1). Additionally, a suitable operating point is located at the point of maximum negative slope in the I/O map, as this corresponds to a good filling level of the evaporator. Slope-seeking and not extremum-seeking control should therefore be used, but the maximum slope is time varying and unknown, and providing the slope-seeking control with the maximum slope as reference makes it unstable, as the slope reduces in both directions of the I/O map.

We previously introduced the idea of searching for a maximum in the derivative or slope of an I/O map in Vinther et al. (2012b) and Vinther et al. (2012c). The novel solution named maximum slope-seeking (MSS) control is closely related to extremum and slope-seeking control, since they all rely on continuous excitation of the system. This excitation provides a means of getting gradient information about the I/O map in the extremum and slope-seeking case and curvature information in the MSS case. At the place of maximum slope, the mean curvature will be zero producing no second harmonic and the second harmonic flips 180° around this point also reflecting the sign of the curvature. This information can be used to drive the system toward the maximum slope of the I/O map. The proposed method is highly non-standard and perhaps non-intuitive and we will need to accept that the superheat will oscillate due to the constant perturbation, which is required to gain the missing information for control purposes in the single sensor setup. However, we are applying a controlled oscillation.

This paper presents the MSS control and provides new single sensor evaporator control results for three widely different refrigeration systems. This includes tests on a supermarket system, and evaluation of the performance compared to a conventional two sensor superheat control. Procedures for system identification and controller tuning is also proposed.

The paper is organized in the following way. Section 2 presents the MSS control method with a simple example simulation and Section 3 describes three different refrigeration system test facilities, which have been used to verify the method. Tuning of the MSS control for refrigeration systems is then treated in Section 5 and the final control setup including necessary safety logic is presented in Section 6. Finally, test results and discussions are presented for each of the test facilities in Section 7 and conclusions are drawn in Section 8.

2. Maximum slope-seeking control

Fig. 2 illustrates the MSS control concept applied to a continuous time process or system with input dynamics $F_i(s)$, an I/O map with sigmoid function properties, and output dynamics $F_o(s)$, constituting a Wiener–Hammerstein model structure ($\mathbb{R}\rightarrow\mathbb{R}$). The goal of the MSS control is to find the desired control signal u^*_{ctrl} that brings the system output $f(u^*_{ctrl})$ to the place of maximum slope in the unknown I/O map.

This is achieved by first of all applying sample S and hold $\mathscr{H}$ on the system and then filtering the sampled system output y with two separate time invariant linear FIR filters $F_1(z)$ and $F_2(z)$, which extracts the coefficients of the first and second harmonics H_1 and H_2 generated by the perturbation sine signal

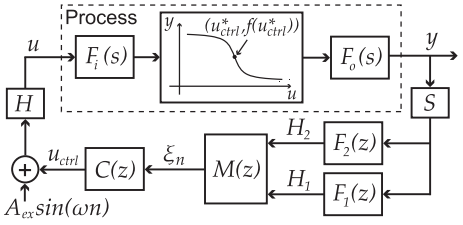

Fig. 2 – MSS control structure applied on a process with a Wiener–Hammerstein model structure.

$A_{ex}\sin(\omega n)$ at the input with amplitude A_{ex} and angular frequency ω. The cross product of vectors in $\mathbb{R}^2$, formed by the coefficients of the harmonics, are then taken and the result is normalized with respect to the first harmonic in $M(z)$, which gives a normalized error signal ξ_n. This error signal will be zero at the desired operating point $f(u^*_{ctrl})$, where the mean curvature is zero, since this gives no second harmonic in the output. The signal will also be positive and negative, respectively, on each side of this point due to the curvature of the I/O map, which is illustrated in Vinther et al. (2012c). An integral controller $C(z)$ is then used to drive the control signal u_{ctrl} toward u^*_{ctrl}. The equations involved in the MSS controller are given in Eqs. (1)–(4).

$$F_1(z) = \frac{2}{N}\sum_{n=1}^{N} z^{n-N}(\cos(\omega(n-N_d)) - j\sin(\omega(n-N_d))), \quad (1)$$

$$F_2(z) = \frac{2}{N}\sum_{n=1}^{N} z^{n-N}(\cos(2\omega(n-N_d)) - j\sin(2\omega(n-N_d))), \quad (2)$$

$$M(z) = \frac{|H_1||H_2|sin(\theta_{12})}{|H_1|^2} = \frac{|H_2|sin(\theta_{12})}{|H_1|}, \quad (3)$$

$$C(z) = \frac{Kt_s}{1-z^{-1}}, \quad (4)$$

where $N = T_{ex}/t_s$ is the number of samples in one perturbation period T_{ex} of ω, t_s is the sample time, N_d is estimated amount of samples equivalent to the delay in the system, θ_{12} is the angle from the first to the second harmonic, and K is the integral gain. The sample time is assumed to be small relative to the perturbation period.

If the dynamics in the system are negligible, compared to the perturbation period T_{ex}, then it is enough to only consider the real part of the second harmonic and use that alone as error signal. In other words, if the phase shift on the second harmonic exceeds 90°, then we would have to change the sign of the feedback. However, avoiding this either requires that the system has fast dynamics or that T_{ex} is very large resulting in a slow feedback loop. Taking the cross product between the harmonic coefficients relates the second harmonic to the first, which means that it is enough to guarantee that only the difference in phase shift, between the first and second harmonic $\Delta\phi_{12}$, is less than 90° (there is already 90° phase shift due to the properties of the harmonics). This means that the time separation between the dynamics and T_{ex} can be lowered. Furthermore, it is possible to compensate for the phase shift introduced by system delay by aligning the cosine and sine terms in Eqs. (1) and (2) with the output by shifting them with the estimated delay samples N_d. This is particularly useful in systems with large delays. For a more detailed description of maximum slope-seeking see Vinther et al. (2012b) and Vinther et al. (2012c).

Simulating an academic example system gives the response shown in Fig. 3. Here we have used Eq. (5) to describe the steady state I/O map

$$y = -k_1 atan(k_2 u), \quad (5)$$

where y is the dimensionless output, $k_1 = 6$ determines the gain in the system, $k_2 = 0.5$ determines the nonlinearity of the system, and u is the dimensionless input. Furthermore, fast

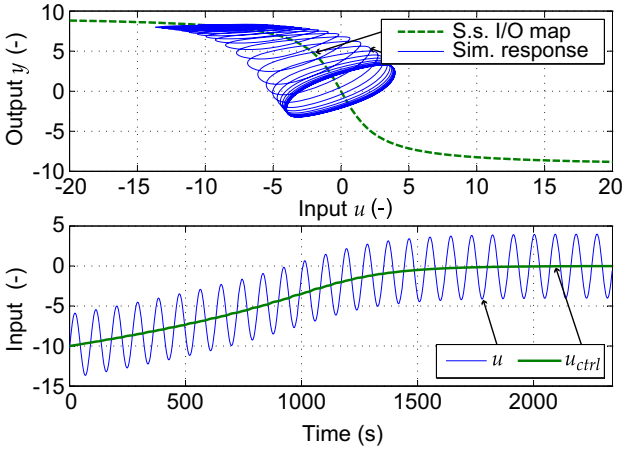

Fig. 3 – MSS control applied to a steady state I/O map with sigmoid function properties. The simulation is started at $u_{ctrl} = -10$ and converges to the desired operating point $u^*_{ctrl} = 0$.

first order dynamics are used in $F_i(s)$ with a time constant of 2 s and first order plus dead time (FOPDT) dynamics are used in $F_o(s)$ with a time constant of 30 s and a relatively large delay of 15 s. The perturbation signal amplitude A_{ex} was set to 4 and the period T_{ex} was set to 3 times the dominant time constant in the system (90 s). Finally, the integral gain was manually tuned and set to $K = 0.05$, with sample time chosen to be $t_s = 1$. Fig. 3 illustrates how the response starts to circle around $u_{ctrl} = -10$ in the I/O map and converges to zero at the maximum slope.

Normalizing the error signal ξ is not a requirement, but using the amplitude of the first harmonic to normalize the error signal gives a way of compensating for changes in system gain. In Eq. (3) we have normalized with the squared amplitude, however, other normalizations such as $|H_1|^{-1}$ or $|H_1|^{-3}$ could have been used as well. Fig. 4 shows the error signal using different normalization at different input offsets or control signals u_{ctrl}, with the example system presented in

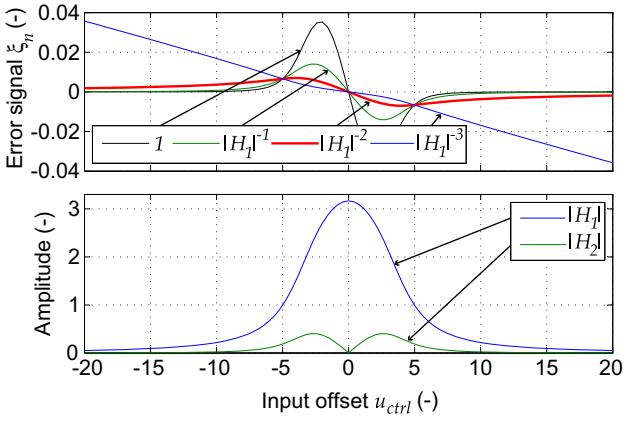

Fig. 4 – Error signal normalized with 1, $|H_1|^{-1}$, $|H_1|^{-2}$, and $|H_1|^{-3}$ at different input offsets, together with the corresponding amplitude of the first and second harmonic.

Fig. 3. The error signal is all positive to the left and all negative to the right of the middle point where the gain in the system is highest. At $u_{ctrl} = 0$ the amplitude of the second harmonic is also zero and the amplitudes are very small when u_{ctrl} gets far from the middle point. The drop in amplitude or system gain could make the control method unstable due to noise and modeling errors, which is also why $|H_1|^{-2}$ in some case is a better normalization than $|H_1|^{-3}$, since the error signal decreases again when the amplitude decreases and thus better resembles how well the Fourier analysis can be trusted. However, remark that Eqs. (1) and (2) acts as a powerful way of filtering out unwanted noise.

3. Test facilities

Three refrigeration system test facilities have been used. The first is a residential air conditioning system, with a max capacity of approximately 11 kW, shown in Fig. 5(a). This system uses refrigerant R410a and has a finned tube evaporator with a pulse-width modulation (PWM) controlled Danfoss Ecoflow™ valve (10 s period). The second system, shown in Fig. 5(b), is a water chiller system with an approximate capacity of 4 kW. This system uses refrigerant R134a and has water on the secondary side of the evaporator and interchangeable valves (either stepper motor EEV or Thermostatic Expansion Valve (TXV)). The last system, shown in Fig. 5(c), is a supermarket refrigeration system with the possibility of connecting a water chiller as additional load. This system uses refrigerant R404a, has PWM controlled valves (6 s period), and has up to two Type 1 and two Type 2 display cases connected. Each display case has a night cover and defrost heater. The compressor rack consists of three compressors, which are controlled separately to keep a set point evaporation temperature T_e and the condenser unit is also set to keep a set point condensation temperature T_c.

These test facilities constitutes a wide variety of refrigeration systems and thus gives a good basis for test of the MSS based single sensor evaporator control. The air conditioning system and the water chiller system is monitored and controlled using the Matlab XPC toolbox for Simulink and the supermarket system uses MiniLog software. They are all sampled at 1 Hz and further information can be found at http://www.es.aau.dk/projects/refrigeration/.

4. Qualitative behavior of evaporator outlet temperature

We are interested in control of the evaporator filling using only the valve OD and the evaporator outlet temperature measurement $T_{e,o}$. Therefore, the steady state I/O map is found using a slow sweep in the input OD from low to high value. This sweep should be stopped when $T_{e,o}$ flattens out again at high OD, when the superheat is low, in order not to let unevaporated refrigerant enter the compressor. However, a small amount of refrigerant spray is tolerable and extra evaporation in the suction line and/or manifold also allows us to have a short period with superheat close to 0 °C. The result for each refrigeration system is shown in Fig. 6.

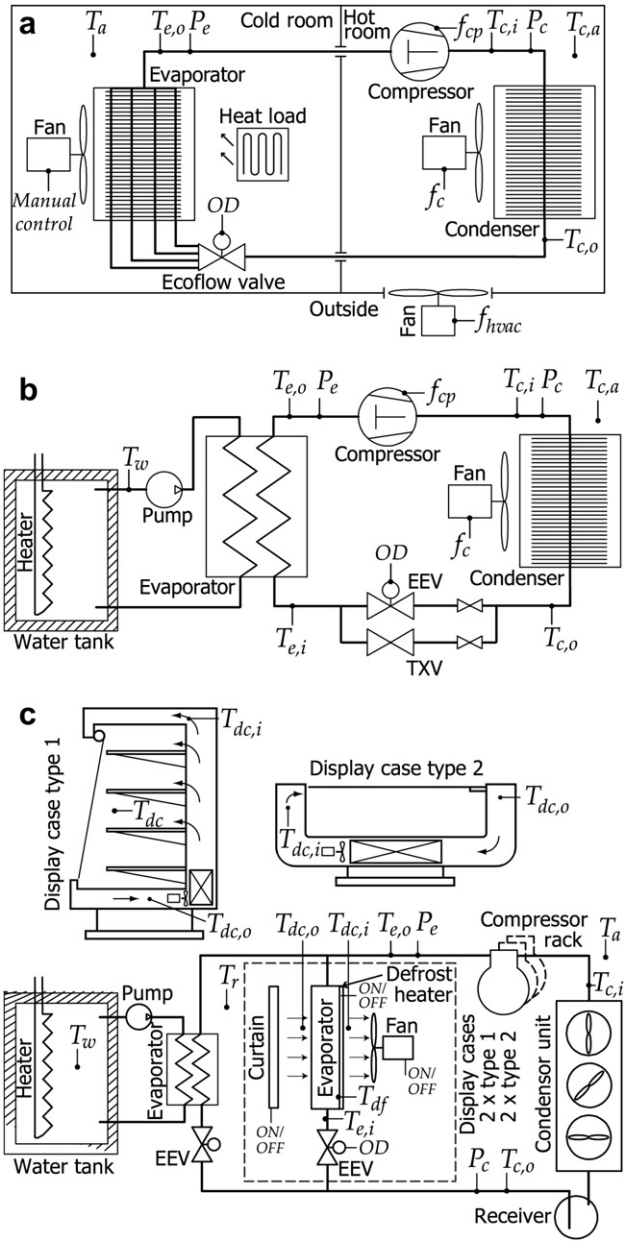

Fig. 5 – Simplified schematics of the air conditioning system (a), the water chiller refrigeration system (b), and the supermarket refrigeration system (c) test facilities with indication of sensors and control signals.

All three evaporators show the same qualitative behavior of the outlet temperature $T_{e,o}$; it has two horizontal asymptotes determined by the temperature of the surrounding medium (air T_a, water T_w) and the evaporation temperature T_e, and a middle temperature where the slope in the system is lowest (negative gain). This point also corresponds to a good superheat or filling level of the evaporator and shows that it is reasonable to search for the point of maximum slope in the I/O map. Note here that if the surrounding temperature or the evaporation temperature changes then it will result in a change in the suitable outlet temperature, which is the main reason for not using a fixed reference. Note also that the

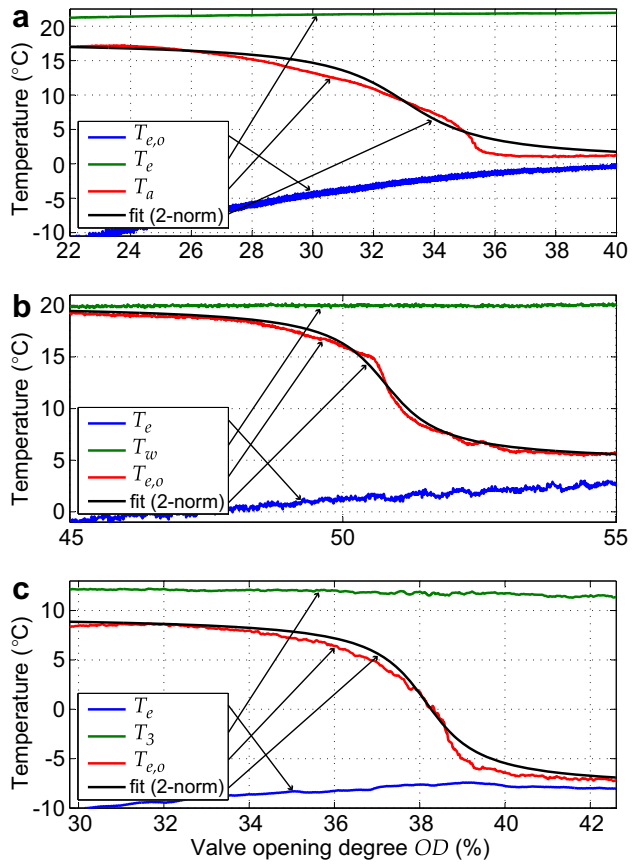

Fig. 6 – Evaporator I/O map revealed by a slow sweep in the input for the air conditioning system (a), the water chiller refrigeration system (b), and the supermarket display case (c). The input is the valve OD and the output is the evaporator outlet temperature $T_{e,o}$. Ambient temperatures are also shown.

typical lumped parameter model used in the literature (see e.g. He et al. (1998)) does not have a smooth S-shape, but rather a sharp corner when $T_{e,o}$ reaches T_e. However, actual evaporator behavior does not exhibit sharp corners because of refrigerant spray and sensor dynamics, because of superposition of separate evaporator sections (investigated in Lyhne and Sørensen (2011)), and because it is a distributed parameter system.

For simulation and controller tuning purposes, models for the steady state I/O map of each refrigeration system is identified. An *atan* function similar to Eq. (5) is used with the expression

$$T_{e,o} = -k_1 atan(k_2(OD + OD^*)) + T^*_{e,o}, \quad (6)$$

since this equation satisfies the sigmoid function properties and because it is relatively easy to fit. The input and output offsets OD^* and $T^*_{e,o}$ also represent the desired operating point and the temperature $T^*_{e,o}$ is determined as

$$T^*_{e,o} = \frac{(T_{e,o,max} + T_{e,o,min})}{2}, \quad (7)$$

where $T_{e,o,max}$ and $T_{e,o,min}$ are the maximum and minimum temperatures during the OD sweep shown in Fig. 6. The valve opening degree OD^* corresponding to $T^*_{e,o}$ is then found and the gain k_1 is given as

$$k_1 = \frac{(T_{e,o,max} - T_{e,o,min})}{\pi} k_3, \quad (8)$$

where k_3 is an optional scaling factor set to 1.1, to add 10% to the gain k_1 in order to account for the fact that $T_{e,o}$ has not reached the horizontal asymptotes yet during the OD sweep. However, conservativeness in controller gain can also account for this model uncertainty, which is why k_3 is optional. The last parameter k_2 is used to fit Eq. (6) to the test data. This is done by using the bisection algorithm on k_2 with an Euclidian error measure. The resulting parameters are listed in Table 1 and the fit is shown in Fig. 6. If the I/O map is not well approximated by a sigmoid function (does not have a unique point of maximum slope), then there is a possibility of having multiple equilibria. However, this has not been experienced with any of the three test setups.

5. Controller tuning

As an overall guideline, the time scales in the controlled system should be:

- Fastest – system dynamics.
- Medium – periodic perturbation.
- Slow – integral control.

The perturbation signal period T_{ex} should be large enough to ensure that any possible change in system dynamics will not result in a difference in phase shift between the two harmonics of more than 90° and large enough to ensure that the perturbation is detectable in the output. The double frequency should also not be a persistent frequency in the noise, since this will directly add to the second harmonic. A suitable large amplitude of the perturbation signal can, however, compensate for the noise. Furthermore, the Fourier analysis implemented with the two filters in Eqs. (1) and (2) are intended for periodic signals, which means that the integral control closing the feedback loop should not be tuned too aggressively. Additionally, if the I/O map has a non-positive first derivative (as in the cases shown in Section 4) then the integral gain K should be positive and negative in the other case. Previously, in Vinther et al. (2012b) and Vinther et al. (2012c), we used PI control instead of just integral control, which made it more difficult to tune the control and the P term can also make the output look less periodic due to jumps in

Table 1 – Evaporator model parameters for the air conditioning, water chiller, and supermarket refrigeration systems.

System	$T^*_{e,o}$	OD^*	k_1	k_2
Air con.	9.08	33.02	5.68	0.50
Chiller	12.41	50.78	4.89	1.31
Supermarket	0.71	38.15	5.59	1.07

the input signal, which results in a poorer estimation of the first and second harmonic.

A method to tune the MSS controller for control of the evaporator filling in a refrigeration system will be given in the following, since the above guidelines are general in their statements. For this purpose a Wiener–Hammerstein model structure, as shown in Fig. 2, is used. It is assumed that the input dynamics F_i can be approximated as being fast and thus negligible compared to the output dynamics (time constant set to 2 s in this paper). Since we already identified the nonlinear I/O map, in Section 4, using an OD sweep on the system, we are left with identifying the output dynamics F_o. A simple way to do this is to perform a relay feedback test around the desired point of operation and approximate the dynamics with a FOPDT model (this approximation is derived in Izadi-Zamanabadi et al. (2012)). However, note that the parameters can vary up to 50% and possibly more (Izadi-Zamanabadi et al., 2012), depending on the characteristics of the used components in the system and the changes in operating conditions. Furthermore, as it can be difficult to separate system nonlinearity from dynamics, we are left with a very rough estimate of the system parameters. Better models could be obtained and more sensor data could be used, but importance have been put in deriving a model with little effort based only on valve input OD and the measured evaporator outlet temperature $T_{e,o}$. Additionally, importance have been put in only using tests that can be automated to ensure that the control setup has a high degree of plug and play (easy to move from system to system).

A biased relay feedback test was performed on each of the three refrigeration systems. The test starts with a low OD to ensure that $T_{e,o}$ is high. However, the starting OD should be high enough to ensure that the compressor does not turn on and off all the time in one-to-one systems (one compressor, one evaporator). A large step up in OD was then made to make the evaporator outlet temperature $T_{e,o}$ drop and OD was stepped back afterward. In order to know when to step back in OD, the rate of change of the temperature $T_{e,o}$ was calculated and filtered and the step was made when a clear peak in the rate of change was detected. A suitable middle temperature was then determined and used as reference for the biased relay feedback test. This test first had three large steps in OD, with the purpose of estimating an OD offset to center three additional relays with smaller amplitude around, providing a better parameter estimate. The last three relays had an amplitude ±10 in OD and a hysteresis on the temperature of 0.5°. Note that only the last relay in the series was used for system identification and one could have taken an average and/or performed more steps.

The ultimate gain K_u is given as (see e.g. Shen et al. (1996))

$$K_u = \frac{4A_i}{\pi A_o}, \tag{9}$$

where A_i is the input step amplitude and A_o is the amplitude of the oscillation in the output. Furthermore, the ultimate period T_u is the time of one relay period. This together with the input and output measurements can be used to calculate the system gain K_{sys} and the system time constant T_{sys} using Eqs. (10) and (11) (see e.g. Shen et al. (1996)).

$$K_{sys} = \frac{\int_{T_u} (T_{e,o}(t) - T_{e,o,ref}(t))dt}{\int_{T_u} (OD(t) - OD_{offset}(t))dt}, \tag{10}$$

$$T_{sys} = \frac{2\pi\sqrt{(K_u K_{sys})^2 - 1}}{T_u}, \tag{11}$$

Finally, there are multiple ways of determining the delay T_d in the system. In this paper we have taken the average time from a step in the input to a change is visible in the output. A detailed review of the biased relay feedback method will not be given in this paper, however, the reader is referred to e.g. Shen et al. (1996) or Wang et al. (1997) for more details.

Fig. 7 shows the relay feedback tests performed on the test facilities. The air conditioning system parameters are $T_{sys} = 23.07$ and $T_d = 15$, the water chiller parameters are $T_{sys} = 31.51$ and $T_d = 26$, and finally the supermarket display case parameters are $T_{sys} = 59.52$ and $T_d = 29$.

The estimated delay can be used for delay compensation ($N_d = \text{round}(T_d)$) and the estimated dominant system time constant T_{sys} can help determine a suitable perturbation time constant T_{ex}. A reasonable value for T_{ex} depends on the confidence in the estimated T_{sys}. With our relatively simple system identification and the large operating point dependence, we will use values between 3 and 5 times the estimated system time constant T_{sys}. The perturbation amplitude A_{ex}

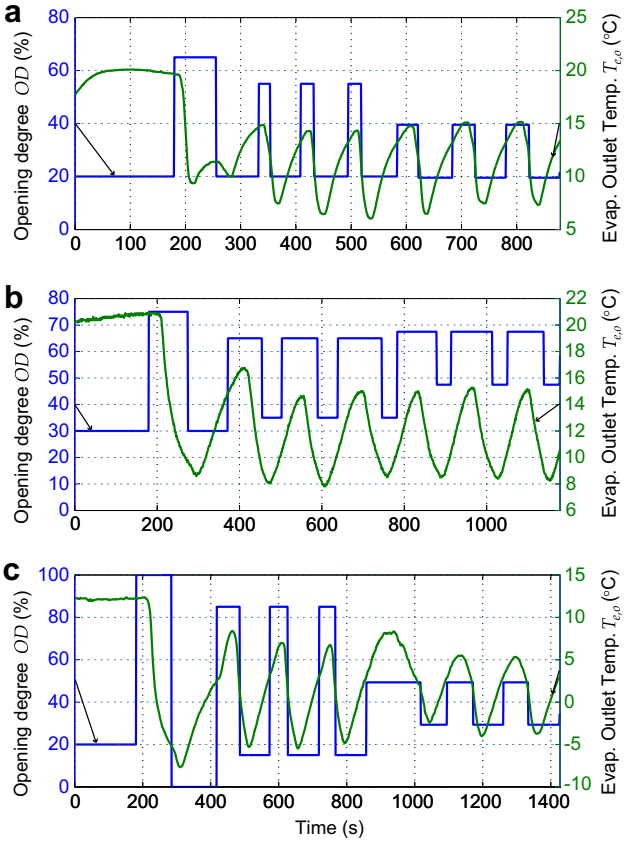

Fig. 7 – Relay feedback test on the air conditioning system (a), the water chiller refrigeration system (b), and the supermarket display case (c).

Table 2 – Chosen perturbation signal values, difference in phase shift between first and second harmonic $\Delta\phi_{12}$, and integral control gain values.

Par.	Air con.	Chiller	Display
T_{ex}	120	130	180
A_{ex}	8.5	10.8	8.0
$\Delta\phi_{12}$	17.13	15.12	12.17
K (neg. start)	0.160	0.136	0.084
K (pos. start)	0.158	0.135	0.085
K (limit)	0.960	0.645	0.468
K (used)	0.079	0.067	0.042

should be as large as possible for robustness, while not exceeding the acceptable level of output excitation. The identified system model can be used to find a suitable A_{ex} and we have used the FOPDT model and iterated A_{ex} until the amplitude of the first harmonic $|H_1|$ is approximately 3, which is acceptable for the three considered refrigeration systems. Finally, we are left with the last MSS control parameter, which is the integral gain K. A possible way to tune K is to use the identified Wiener–Hammerstein model and iterate K until the desired response is achieved. In this paper a convergence test is used and K is iterated until the response have an overshoot of 10%. If the starting value of u_{ctrl} is 10 larger than the value at the desired operating point u^*_{ctrl}, then it corresponds to allowing 1% OD overshoot. Both a negative and a positive convergence test is made and half of the smallest K value is used to account for model uncertainty. Additionally, the stability limit on the gain K is checked when the system is started at the desired operating point u^*_{ctrl}, where the system gain is highest.

The chosen control parameters and identified control gains for the three refrigeration systems are listed in Table 2. The perturbation signal period T_{ex} is approximately five times, four times, and three times the system time constant for the air conditioning system, water chiller system, and the supermarket display case system, respectively. This gives in all cases a difference in phase shift much lower than the limit of 90°. Furthermore, the stability limit on K is much higher than the value obtained in the convergence tests and correspondingly the value used in the tests presented in Section 7.

6. Control setup and safety logic

The MSS setup applied to a refrigeration system for single sensor evaporator control is illustrated in Fig. 8. The valve OD

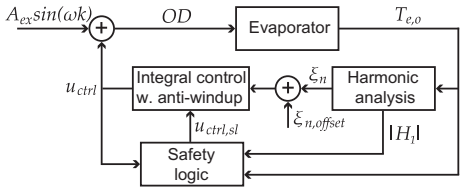

Fig. 8 – MSS control setup with safety logic applied to a refrigeration system evaporator. The harmonic analysis block includes the filters F_1 and F_2 and the normalized crossproduct operation (see e.g. Fig. 2). When the safety logic is activated u_{ctrl} is replaced by $u_{ctrl,sl}$.

input is limited between 0 and 100%, which means that the control signal must be within the limits $A_{ex} \le u_{ctrl} \le 100 - A_{ex}$, to leave space for the perturbation. Anti-windup is therefore added to the integral control.

The normalized error signal ξ_n is calculated based on measurement of the excited evaporator outlet temperature $T_{e,o}$. An offset $\xi_{n,offset}$ can be added to lift or lower the outlet temperature if the point of maximum slope lies too close or too far away from a suitable filling of the evaporator. In the air conditioning system and the supermarket system a small offset has been added to lift $T_{e,o}$ one to two degrees. $\xi_{n,offset}$ was set to −0.1 and −0.05 for the air conditioning system and the supermarket display case, respectively. The value can e.g. be determined based on the same simulation that was used to find the integral gain K.

An important note to make is that the cost of adding an offset is that the system will not stabilize at the desired operating point if the input gets far from the desired operating point, which can be deduced from Fig. 4. Lowering the error signal means that low values of u_{ctrl} will not result in a positive error signal as required. Safety logic is therefore added in order to solve this problem, which occurs when the amplitude of the first harmonic is low. The role of the safety logic is to monitor the amplitude of the first harmonic. If this amplitude is consistently below a threshold, a step back in u_{ctrl} is made to ensure that we are in the low flow situation and u_{ctrl} is then ramped up until the amplitude gets above an upper threshold again. A flow diagram is shown in Fig. 9 which illustrates the safety logic. Another benefit of having the safety logic is that

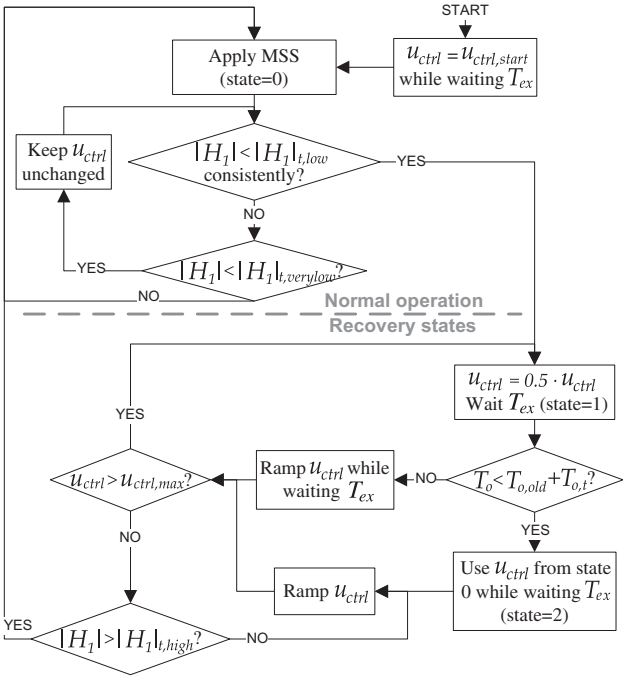

Fig. 9 – Safety logic illustrated with a flowchart. State 0 indicates normal operation, state 1 is recovery from evaporator overflow and state 2 is recovery from low refrigerant flow situation. A sine signal is always superimposed on the control signal u_{ctrl} giving the applied valve OD.

low refrigerant flow or evaporator overflow is quickly detected and taken care of, even if the feedback loop is tuned conservatively. The outlet temperature is monitored when a step back in u_{ctrl} is made to determine if the low amplitude was caused by a low flow or an overflow situation. In the low flow situation u_{ctrl} can be stepped back up and ramped from there instead.

The wait periods that allows the system to settle after steps in u_{ctrl} are dependent on the particular perturbation period T_{ex}. The thresholds $|H_1|_{t,very\ low}$, $|H_1|_{t,low}$, and $|H_1|_{t,high}$ depends on the amplitude A_{ex}, which was adapted to give the same excitation in the three systems. The thresholds were set to 0.33, 1.5, and 2, respectively, for the air conditioning and the water chiller systems, which are one compressor one evaporator systems. The values for the supermarket system was set a little lower at 0.33, 1 and 1.5. Furthermore, the amplitude $|H_1|$ was considered consistently low after $0.67T_{ex}$ and the ramp rate was set to $0.5A_{ex}/T_{ex}$. Finally, the temperature threshold $T_{o,t}$ used to detect low flow situations was set to 4 °C. The safety logic parameters can be adjusted to give the desired sensitivity toward low flow or overflow situations, but they are not that important if the error signal offset is zero and the control can be tuned non-conservatively.

7. Results and discussions

The single sensor MSS control with safety logic has been tested on each of the three refrigeration systems.

7.1. *Water chiller refrigeration system test*

Fig. 10 shows the test result from an 8 h and 20 min test conducted on the water chiller refrigeration system. The condensation pressure was controlled separately with a PI controller on the condenser fan, with the reference $P_{c,ref} = 9$ bar. The compressor frequency was changed in steps between the four levels 60, 45, 35, and 30 Hz. This gives large disturbances in the evaporation temperature and the heat load was additionally changed between approximately 2.8 kW and 3.6 kW with a constant water mass flow of 0.31 l s^{-1}. The chosen disturbance pattern is based on the test description in Izadi-Zamanabadi et al. (2012) and equal to the test conducted in Vinther et al. (2012b). This makes it possible to compare the proposed MSS control setup and safety logic with previous results and the TXV result obtained in Vinther et al. (2012b), which is also shown in Fig. 10.

The top graph in Fig. 10 shows the control signal u_{ctrl}, which was stepped back four times during the test by the safety logic. The first time was in the start because the starting OD was too low giving a low flow situation. Then two overflow situations were detected after the largest step down in compressor frequency and approximately 5.5 h into the test. Finally, the largest step up in compressor frequency caused a low flow situation. A safety logic activation causes a period of approximately 15 min with higher superheat before the control converges again, however, the average superheat for the whole test was $\overline{T}_{sh,mss} = 12.90$ °C, which is very close to the superheat obtained with the TXV valve $\overline{T}_{sh,txv} = 12.68$ °C. If comparing the superheat when the safety logic is not activated with the TXV result, then lower superheat is obtained with the single sensor MSS controller.

An important thing to remember is that the single sensor MSS control maintains a low average superheat during the entire test without actually measuring the superheat. A requirement though is that the system is continuously perturbed, which results in higher fluctuations in the superheat. However, this fluctuation is not visible in the water temperature T_w (or in the air temperature in the following tests on the other two systems). Using a fixed outlet temperature reference would not be possible as the average outlet temperature varies between 6 °C and 12.4 °C in the test. This is mainly because of changes in water temperature, which were $T_w = 14.65$ and $T_w = 20.8$ °C in the two cases.

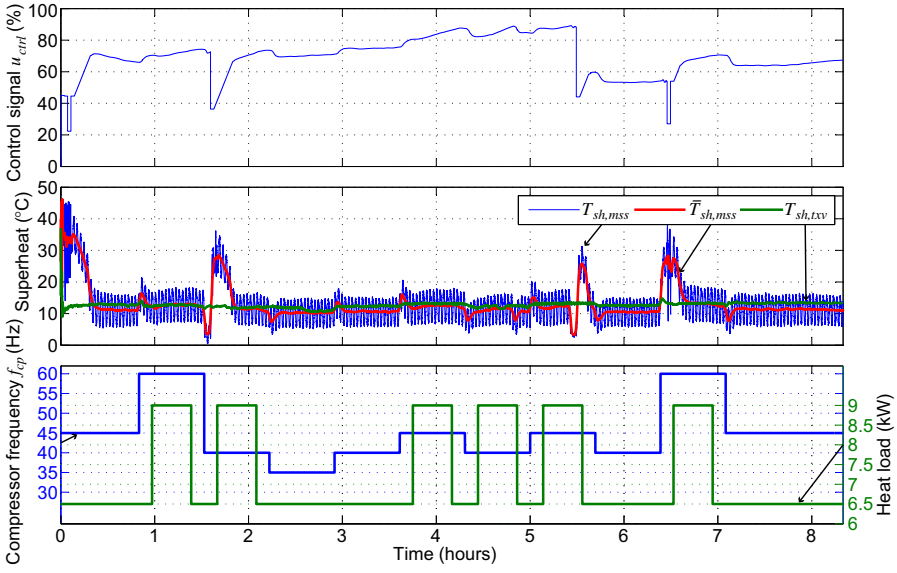

Fig. 10 – Test result with MSS applied on the water chiller refrigeration system for single temperature sensor evaporator filling control. Average superheat obtained with the TXV instead of MSS is shown for comparison.

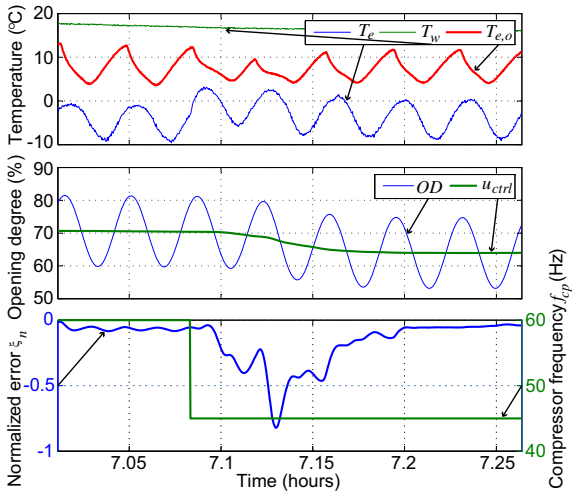

Fig. 11 – Small part of the test result shown in Fig. 10. Two periods before and five periods after a step down in compressor speed.

A small part of the 8 h and 20 min test is shown in Fig. 11. The top graphs shows the excited evaporator outlet temperature $T_{e,o}$ in between the water temperature T_w and the evaporation temperature T_e. The bottom graph shows how the step down in compressor frequency results in a change in the normalized error signal that decreases u_{ctrl}, which is the correct response, since the refrigerant mass flow is lowered.

7.2. Air conditioning system test

Fig. 12 shows a similar test conducted on the air conditioning system. The condensation pressure was again controlled separately to the reference $P_{c,ref} = 24$ bar. In this test the compressor frequency was stepped up and down between the levels 50, 42.5, 35, and 25 Hz and the heat load was changed between 4.5 and 9 kW with the air flow across the evaporator set to approximately 66% of max.

The average superheat for the whole test was $\overline{T}_{sh,mss} = 7.90$ °C and the safety logic was only activated once when the compressor frequency was stepped down to the lowest level. This is an improvement compared with the result obtained in Vinther et al. (2012b), where the safety logic was activated 5 times and the average superheat was 10.31 °C. This is mainly achieved by lowering the perturbation period from 180 to 120 s made possible with the delay compensation and the small offset in the normalized error signal.

7.3. Supermarket refrigeration system tests

The condensation pressure was controlled separately in all the tests on the supermarket refrigeration system giving an almost constant condensation temperature $T_c = 35$ °C. Additionally, a controller on the compressor rack ran with an evaporation temperature reference $T_{e,ref} = -15$ °C. The compressor rack consists of three compressors with max power consumption of 4, 6, and 13 kW (delivered power to compressor). The controller switches the total power consumption of the rack in steps of approximately 1.1 kW. This gives large variations in evaporation temperature T_e.

Fig. 13 shows the test result of a test conducted on the supermarket refrigeration system. Single temperature sensor MSS control was applied on one Type 1 display case (see Fig. 5(c)) and another Type 1 display case had a conventional two sensor superheat controller with temperature control. The valve on/off behavior of the second display case gives large disturbances in the evaporation temperature, which is shown in the bottom graph. This causes the compressor rack to shift between five levels (approx. 1.1–5.5 kW). However, in spite of the disturbances an average superheat of $\overline{T}_{sh,mss} = 8.81$ °C is still maintained.

Four low flow situations are encountered in the middle of the test between 5 and 6 h, but they are handled by the safety

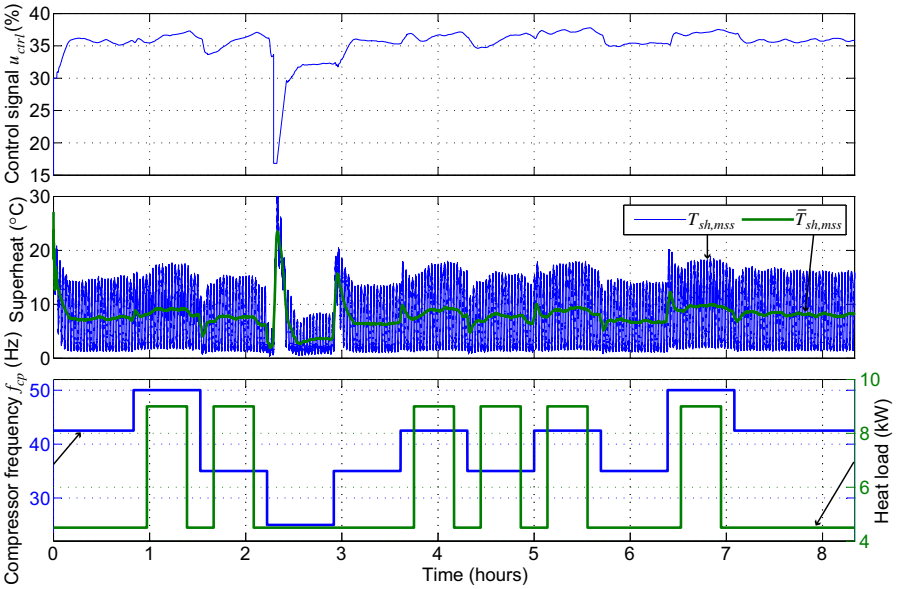

Fig. 12 – Test result with MSS applied on the air conditioning system for single temperature sensor evaporator filling control.

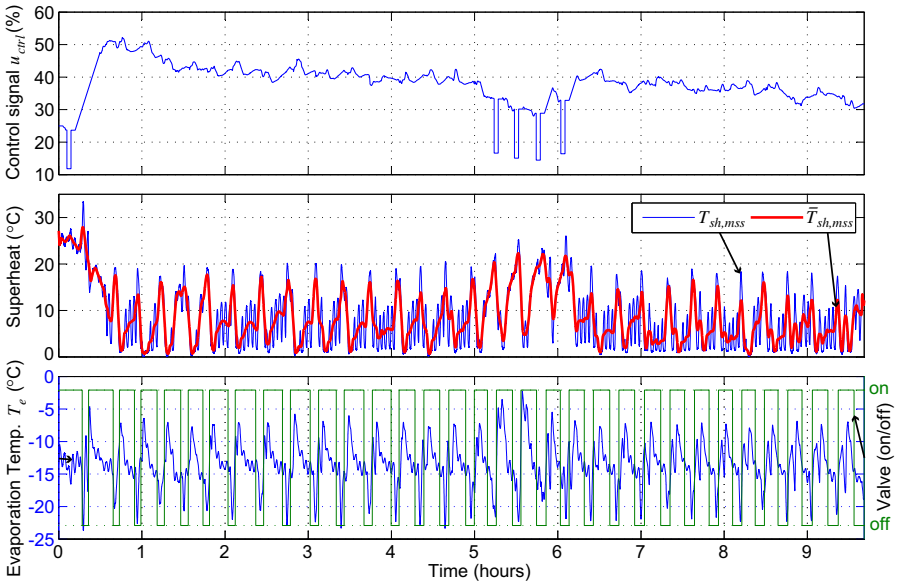

Fig. 13 – Test result with MSS applied on the supermarket refrigeration system display case for single temperature sensor evaporator filling control. Valve (on/off) refers to a secondary display case running conventional two sensor superheat control with temperature control, which gives large evaporation temperature disturbances.

logic. A gradual frost build up in the evaporator causes the control signal u_{ctrl} to slowly decrease, since the defrost algorithm is deactivated, which causes a decrease in heat transfer.

Two tests have been conducted in order to compare the performance of the single sensor MSS control against the conventional two sensor superheat control (both controllers use an EEV). Only one display case was connected to the supermarket refrigeration system during the test and each test included two different operating conditions (with and without night cover). The superheat during the tests is presented in Fig. 14. The average superheat during the period without cover is $\overline{T}_{sh,mss} = 6.83$ for the single sensor control and $\overline{T}_{sh,conv} = 11.56$ for the two sensor control and with cover it is $\overline{T}_{sh,mss} = 7.54$ and $\overline{T}_{sh,conv} = 12.19$. The superheat is considerably lower in the MSS case, which means a better utilization of the evaporator and potentially higher cooling capacity. This does not necessarily give a better COP and longer tests in a climate controlled chamber with power measurements would be required, before a conclusion can be made about any long term economic difference in the two methods. However, preliminary tests have indicated that the methods are comparable in terms of efficiency.

Finally, the single sensor MSS is tested together with valve on/off temperature control. The on/off control is implemented so that it opens the valve fully for a short period after an off period in order to quickly refill the evaporator. The full opening is stopped and MSS control is started when a clear peak in the rate of change of $T_{e,o}$ is detected (same procedure as in the start of the relay test, see Section 5). Fig. 15 shows the control signal u_{ctrl}, the valve OD, the achieved superheat T_{sh}, and the display case temperature T_{dc} (hysteresis 0–5 °C). The on versus off period is approximately equal and the on period is barely long enough for the single sensor MSS control to take effect, but it does optimize and maintain a reasonable

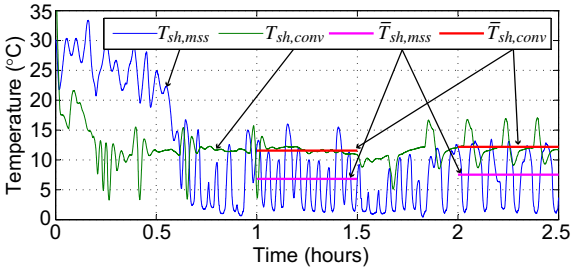

Fig. 14 – Superheat and average superheat during two separate but equivalent tests on the supermarket refrigeration system with MSS and conventional control, respectively. The average values are calculated between 1 and 1.5 h (no cover) and 2–2.5 h (cover).

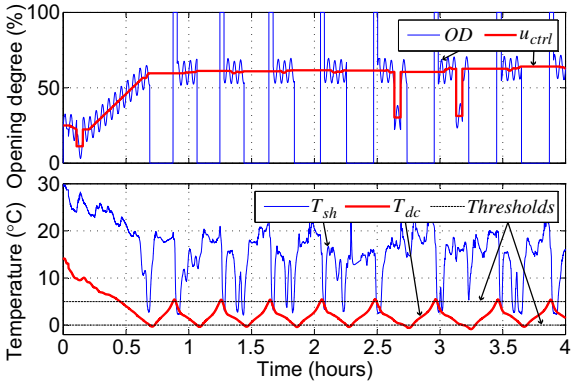

Fig. 15 – MSS with valve on/off control on the display case temperature in the supermarket refrigeration system.

superheat when the valve is on. Better performance can be obtained if the on period is made longer.

8. Conclusion

Tests on three widely different refrigeration systems have shown, that it is possible to control the superheat or filling of the evaporator to a suitable level, using only a single temperature measurement combined with an EEV. A novel MSS method has ensured that this level could be obtained and the method relies on continuous perturbation of the system. This perturbation generates higher harmonics in the output due to the curvature of the I/O map and these harmonics can then be used to drive the system toward the point of maximum slope, where the mean curvature is zero. Additional safety logic was added to ensure faster recovery from low flow or overflow situations.

Long tests with disturbances have shown the robustness of the method. The single sensor solution had a considerably lower average superheat, which can give a higher cooling capacity. A final test showed that the display case temperature in a supermarket refrigeration system can be controlled simultaneously.

A tuning approach for the MSS controller has also been provided. The tuning relies on a slow OD sweep together with a relay feedback test. These tests only have to be run the first time the control is used and can be implemented to run automatically. Furthermore, the control method does not rely on a system model and is believed to have a high degree of plug and play potential. The only requirement is that the system under consideration can be approximated by a sigmoid function, and that the desired operating point is located at the point of maximum slope.

Acknowledgments

The authors gratefully acknowledge financial support from the Faculty of Engineering and Science at Aalborg University, the Danish Council for Independent Research – Technology and Production Sciences, and Danfoss A/S.

REFERENCES

Ariyur, K.B., Krstic, M., 2003. Real-time Optimization by Extremum-seeking Control. Wiley-Interscience.

Dincer, I., Kanoglu, M., 2010. Refrigeration Systems and Applications, second ed. Wiley.

Elliott, M.S., Rasmussen, B.P., 2010. On reducing evaporator superheat nonlinearity with control architecture. Int. J. Refrigeration 33 (3), 607–614.

Finn, D.P., Doyle, C.J., 2000. Control and optimization issues associated with algorithm-controlled refrigerant throttling devices. ASHRAE Trans. 106 (1), 524–533.

He, X., et al., 1998. Multivariable control of vapor compression systems. HVAC&R Res. 4 (3), 205–230.

Henning, I., et al., 2008. Extensions of adaptive slope-seeking for active flow control. Proc. IMechE, Part. J. Syst. Control Eng. 222 (5), 309–322.

Izadi-Zamanabadi, R., Vinther, K., Mojallali, H., Rasmussen, H., Stoustrup, J., 2012. Evaporator unit as a benchmark for Plug and Play and fault tolerant control. In: 8th IFAC Symposium on Fault Detection, Supervision and Safety of Technical Processes. Mexico City, Mexico, pp. 701–706.

Li, X., Li, Y., Seem, J. E., Li, P., 2012. Extremum seeking control of cooling tower for self-optimizing efficient operation of chilled water systems. In: American Control Conference. Montreal, Canada.

Lyhne, C.H., Sørensen, E.B., 2011. Generic Superheat Control of Evaporators using One Sensor and One Actuator. Aalborg University, Denmark. Master thesis.

Moase, W.H., Manzie, C., 2011. Fast extremum-seeking on Hammerstein plants. In: 18th IFAC World Congress. Milan, Italy, pp. 108–113.

Moir, T.J., 2001. Automatic variance control and variance estimation loops. Circuits Syst. Signal. Process 20 (1), 1–10.

Rasmussen, H., 2008. Nonlinear superheat and capacity control of a refrigeration plant. In: 17th IEEE International Conference on Control Applications. San Antonio, Texas, USA, pp. 97–101.

Sane, H.S., Haugstetter, C., Bortoff, S.A., 2006. Building HVAC control systems – role of controls and optimization. In: American Control Conference. Minneapolis, Minn., USA, pp. 1121–1126.

Schurt, L.C., Hermes, C.J., Neto, A.T., 2009. A model-driven multivariable controller for vapor compression refrigeration systems. Int. J. Refrigeration 32 (7), 1672–1682.

Shen, S.-H., Wu, J.-S., Yu, C.-C., 1996. Use of biased-relay feedback for system identification. AIChE J. 42 (4), 1174–1180.

Vinther, K., Lyhne, C.H., Sørensen, E.B., Rasmussen, H., 2012a. Evaporator superheat control with one temperature sensor using qualitative system knowledge. In: American Control Conference. Montreal, Canada, pp. 374–379.

Vinther, K., Rasmussen, H., Izadi-Zamanabadi, R., Stoustrup, J., 2012b. Single temperature sensor based evaporator filling control using Excitation signal harmonics. In: IEEE Multi-conference on Systems and Control. Dubrovnik, Croatia, pp. 757–763.

Vinther, K., Rasmussen, H., Izadi-Zamanabadi, R., Stoustrup, J., 2012c. Utilization of excitation signal harmonics for control of nonlinear systems. In: IEEE Multi-conference on Systems and Control. Dubrovnik, Croatia, pp. 1627–1632.

Wang, Q.-G., Hang, C.-C., Zou, B., 1997. Low-order modeling from relay feedback. Ind. Eng. Chem. Res. 36 (2), 375–381.

Zhang, C., Ordez, R., 2012. Extremum-seeking Control and Applications: a Numerical Optimization-based Approach. In: Advances in Industrial Control. Springer.